KU ScholarWorks

Measurement of the branching ratio for the decay τ→e⁻–v⁻(e)v(τ)

Item Type	Article
Authors	Baringer, Philip S.
Citation	Baringer, Philip S. et al. (1990). "Measurement of the branching ratio for the decay τ→e⁻–v⁻(e)v(τ)." Physical Review D, 1990(41):1414. http://dx.doi.org/10.1103/PhysRevD.41.1414
DOI	10.1103/PhysRevD.41.1414
Publisher	American Physical Society
Download date	2024-07-30 16:36:34
Link to Item	http://hdl.handle.net/1808/15247

Measurement of the branching ratio for the decay $\tau^- \to e^- \bar{\nu}_e \nu_\tau$

S. Abachi,* M. Derrick, P. Kooijman,† B. Musgrave, L. Price, J. Repond, and
K. Sugano
Argonne National Laboratory, Argonne, Illinois 60439

D. Blockus, B. Brabson, J.-M. Brom,‡ C. Jung,§ H. Ogren, and D. R. Rust
Indiana University, Bloomington, Indiana 47405

B. Cork
Lawrence Berkeley Laboratory, Berkeley, California 94720

C. Akerlof, J. Chapman, D. Errede,** M. T. Ken, D. I. Meyer, H. Neal,
D. Nitz, R. Thun, and R. Tschirhart*
University of Michigan, Ann Arbor, Michigan 48109

P. Baringer,†† B. G. Bylsma,‡‡ R. DeBonte, D. Koltick, E. H. Low,§§ R. L. McIlwain,
D. H. Miller, C. R. Ng, and E. Shibata
Purdue University, W. Lafayette, Indiana 47907
(Received 1 August 1989)

This paper reports a new measurement of the branching ratio for the decay $\tau^- \to e^- \bar{\nu}_e \nu_\tau$. The data were taken with the High Resolution Spectrometer at the SLAC e^+e^- colliding-beam facility PEP, operating at $\sqrt{s} = 29$ GeV. The result $B(\tau^- \to e^- \bar{\nu}_e \nu_\tau) = (17.0 \pm 0.5 \pm 0.6)\%$, together with our measurements of the lifetime and the topological branching fractions of the τ lepton are compared with theoretical expectations.

I. INTRODUCTION

Since its discovery[1] in 1975, the properties of the τ lepton have been studied extensively at all e^+e^- colliders having a center-of-mass energy above the production threshold. The measurements of its spin, production, and decay properties all indicate that the τ is the sequential lepton of the third generation.[2] However, experiments have not yet proven this view, and conceivably, interactions of the τ lepton may still differ from the $V-A$ postulated in the standard model.[3] Such deviations could be detected through measurements of the lepton universality, i.e., comparison of the lifetime and decay branching ratios of the τ, or the measurements of the Michel parameter in the lepton decay modes. Therefore, precision measurements of the production and decay properties of the τ lepton are of utmost importance and could lead to exciting surprises.

In fact, a strong specific motivation for the study of the properties of the τ lepton is generated by the long-standing discrepancy between the inclusive decay branching fraction into one charged particle and the sum of the exclusive one-prong final states. This problem was first noticed by Truong[4] in 1984, and despite recent precise measurements of the quantities involved, no convincing solution has emerged.

Using world-average values,[5] the decay branching fraction into one charged particle is measured to be $B_1 = (86.0 \pm 0.3)\%$, whereas the sum of the exclusive modes with one charged particle is $S_1 = (78.2 \pm 1.8)\%$. Including theoretical limits on unmeasured rare decay modes yields $S_1 < (80.4 \pm 1.8)\%$. Therefore, the difference between the inclusive and exclusive measurement is $\Delta = B_1 - S_1 > (5.6 \pm 1.8)\%$, which corresponds to a three standard deviation effect. If the sum over the exclusive modes is calculated replacing the poor measurement of the decay rate for $\tau^- \to \pi^- \pi^0 \pi^0 \nu$ by the relatively well-measured rate for the decay $\tau^- \to \pi^- \pi^+ \pi^- \nu$,[6] the effect is even more pronounced, $\Delta > (6.3 \pm 1.3)\%$.

In this paper we report a new measurement of the decay rate of the τ lepton into electrons $B_e = B(\tau^- \to e^- \bar{\nu}_e \nu_\tau)$ based on data recorded by the High Resolution Spectrometer (HRS) at the SLAC e^+e^- colliding-beam facility PEP. The data, corresponding to an integrated luminosity of about 300 pb^{-1}, were collected over a period of 5 yr at a center-of-mass energy $\sqrt{s} = 29$ GeV.

The result of this measurement has already been published;[7] the present paper completes the discussion of the data taking and event selection and describes the analysis methods in detail. Particular attention has been paid to understanding systematic errors.

In the final section, we compare our measurement of the decay rate into electrons with theoretical predictions based on recent HRS measurements of the lifetime and the topological decay branching fractions of the τ lepton.

II. APPARATUS AND DATA TAKING

A. Apparatus

Detailed descriptions of the detector systems and the performance of the HRS appear elsewhere,[8] so only a

brief outline will be repeated here. The elements of the detector, as shown in Fig. 1, were all located within the large solenoidal magnetic field volume (4.45 m in diameter and 4.0 m in length) providing a central magnetic field of 1.62 T. In order of increasing radius, the detector system consisted of the vertex detector, central drift chamber, Čerenkov counters, outer drift chamber, and the barrel calorimeter. The forward and rear ends were covered with end-cap calorimeters. The detectors used in the present work are the central and outer drift chambers and the barrel calorimeter.

The momenta of charged tracks were measured with excellent resolution, $\sigma_p/p = 0.002p$ (p in GeV/c) for high-momentum tracks. This is achieved by the following.

(a) A thin front end: The total thickness of material from the beam line to the middle layer of the central drift chamber was only 0.017 in radiation length.

(b) A large tracking volume: The central drift chamber had 15 layers extending in radius from 0.2 to 1.0 m and includes eight stereo and seven axial layers. The outer drift chamber consisted of two layers of tubes at a radial distance of 2.0 m from the beam axis.

(c) A homogeneous magnetic field: In the region of the central drift chamber the field was uniform to 1% and to 3% over the whole inner volume.

The present analysis depends on the barrel shower-counter system for the identification of electrons. It consisted of 40 modules[9] constructed with alternate layers of lead and scintillator, with each module subtending an angle of 9° in azimuth. The modules were segmented in depth into a $3X_0$ and an $8X_0$ section with a single layer of 14 proportional wire chambers separating the two regions, as shown in Fig. 2. The layer of proportional wire chambers was at a radius of 2.03 m from the e^+e^- beam axis. The energy resolution of the shower counters can be parametrized as

$$\left[\frac{\sigma_E}{E}\right]^2 = \frac{0.16^2}{E} + 0.06^2 + 0.011^2 E \quad (E \text{ in GeV}) , \quad (1)$$

where the first term represents the sampling fluctuations,

FIG. 1. Overview of the High Resolution Spectrometer.
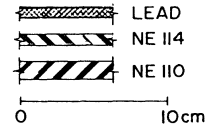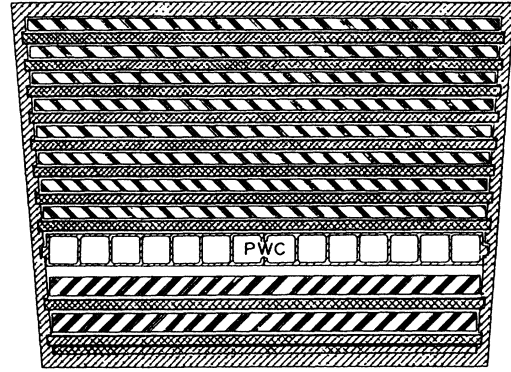

FIG. 2. Cross section through a barrel shower-counter module.

the second term the calibration systematics, and the last term shower leakage. The z position of a shower, along the beam axis, was determined by current division in the wire chambers to an accuracy of $\sigma_z = 2.5$ cm.

The calibration of the barrel shower-counter system for energy, time-of-flight, and shower position was achieved using calibration data from colliding-beam QED events: Bhabha scattering, radiative Bhahba events, γ pairs, μ pairs, and τ pairs. The tracking provided well-measured momenta and positions of entry into the barrel, so that the particles from these events have known energies, shower positions, and flight times.

The HRS was stable and reliable in operation. For example, the fraction of inoperative drift-chamber cells during experimental running was typically less than 1% and the barrel calorimeter operated with virtually no downtime.

B. Data taking

The data were collected during a 5-yr running period from 1981 to 1986 at a center-of-mass $\sqrt{s} = 29$ GeV. The integrated luminosity was measured by counting both wide-angle Bhabha events[10] and τ-pair events.[11] The error on the integrated luminosity as determined by counting wide-angle Bhabha events is dominated by the uncertainty in the efficiency calculation related to the electron identification techniques. The error on the integrated luminosity as determined by counting τ-pair events is dominated by the limited statistics of the data sample and the uncertainty in the efficiency calculation introduced by the missing one-prong problem. The results are

$$\int L \, dt_{\text{Bhahba}} = 291 \pm 7 \text{ pb}^{-1} ,$$

$$\int L \, dt_{\tau \text{ pair}} = 304 \pm 7 \text{ pb}^{-1} .$$

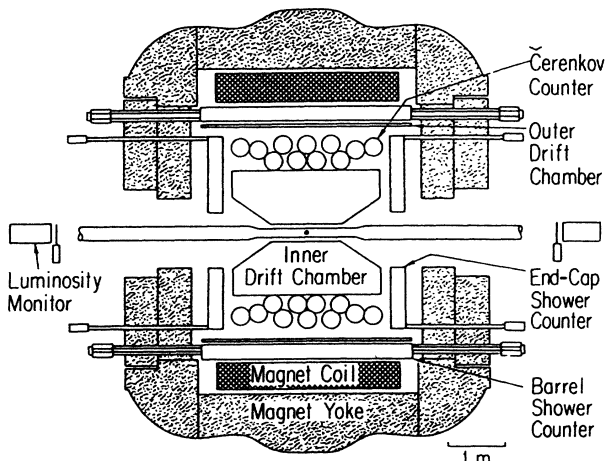The two measurements are independent, and so we use

their weighted average value for the integrated luminosity of the experiment:

$$\int L \, dt_{\text{average}} = 298 \pm 5 \text{ pb}^{-1} \, .$$

All candidate events were required to satisfy at least one of the three neutral-energy and/or charged-track triggers: (a) neutral energy $E > 4.8$ GeV; (b) $E > 2.4$ GeV and at least one track reconstructed by the hardware track processor; (c) two or more reconstructed tracks, at least one of which was in time with the beam crossing. Most of the τ-pair events satisfy both trigger conditions (a) and (b). The trigger efficiency for two-prong events of $(99.93 \pm 0.01)\%$ was measured using Bhabha events, since they always satisfied both the charged trigger and the neutral trigger. The efficiencies for the higher-multiplicity topologies are even higher.

III. τ-PAIR EVENT SELECTION

At a center-of-mass energy $\sqrt{s} = 29$ GeV τ-pair production yields final states with clear back-to-back topologies and so excellent separation of the charged tracks and neutral energy clusters from the decays of the two τ leptons. For the measurement of the branching ratio of the decay $\tau^- \rightarrow e^- \bar{\nu}_e \nu_\tau$, events are selected where one charged track recoils either against one oppositely charged track (1-1 charged topology) or one oppositely charged jet of three charged tracks (1-3 charged topology). In order to assure proper electron identification, the single tracks were required to have momenta exceeding 1.0 GeV/c and to enter the barrel shower-counter modules inside a fiducial volume that is 30 cm from either end and 1.7 cm from each intermodule boundary.

The potential backgrounds to the τ-pair sample come from many different sources: Bhabha events, radiative Bhabha events, μ-pair events, two-γ events (for example, $e^+ e^- \rightarrow e^+ e^- \mu^+ \mu^-$), hadronic events, cosmic rays, and beam-gas events. The selection criteria were devised to efficiently suppress all background contaminations, while retaining the largest fraction of signal events.

Two-γ events were suppressed by accepting only events with a scalar sum of the charged momenta above 7.25 GeV/c and an acollinearity angle between the two jets of less than 45°. Beam-gas events and cosmic rays were rejected by a vertex cut: the distance of closest approach of any track to the interaction point was required to be less than 1 cm radially and less than 9 cm along the beam direction. In addition, for events with a 1-1 charged topology, the time of flight for each track had to be within 3 ns of the expected time. Bhabha events and μ pairs were rejected by requiring that the scalar sum of the charged momenta be less than 23.2 GeV/c and that no jet had a momentum exceeding 13.0 GeV/c. In addition, specifically for 1-1 events, the total energy measured by the barrel shower counter was required to be less than half the center-of-mass energy.

Further selection cuts were applied to the events with a 1-1 topology, depending on the number of electron candidates found. An electron candidate is defined as a track with an associated shower energy E exceeding 3 GeV/c

or an E/p ratio larger than 0.5, where p is the momentum of the track. Events with two electron candidates were rejected, as they are likely to be Bhabha events. The momenta of the tracks from events with no electron candidate were required to be below 11 GeV/c, which efficiently reduces the μ-pair contamination.

In the 1-3 topology, the background from low-multiplicity hadronic events was reduced by requiring that the invariant mass of the three-track jet be less than 1.6 GeV/c^2. Finally, radiative Bhabha events with a converted photon, resulting in an event with a 1-3 topology, were rejected by requiring that no more than one jet track deposits a shower energy E corresponding to an E/p ratio larger than 0.9.

These data selections yield 3628 events in the 1-1 topology and 2269 events in the 1-3 topology. The remaining backgrounds are dominated by two-γ events in the 1-1 topology and by low-multiplicity hadronic events in the 1-3 data sample.

IV. DETERMINATION OF THE NUMBER OF ELECTRONS IN THE τ-PAIR EVENT SAMPLE

Electrons are identified through the measurement of their associated electromagnetic showers in the barrel shower counter and by comparing the deposited energy to the measured track momentum. Two different approaches were followed to extract the number of electrons in the data sample: the first utilizes the E/p ratio with the energy taken as the sum of the measurements of the inner and outer segmentation of the shower-counter modules, and the second is based on the definition of a χ^2 that uses the separate information from the two segmentations in depth.

A particular effort was made to minimize the systematic errors due to an imperfect Monte Carlo simulation of the experiment on the level of both the event generation and the detector simulation. Therefore, instead of relying on a parametrized simulation of the detector response to determine the signature of electrons in the τ-pair data sample, we used a clean sample of electrons from selected radiative Bhabha events and two-γ events containing two electrons in the final state. This procedure results in a more reliable parametrization of the electron signal, in particular in a precise description of the tails of the distributions. Furthermore, the background in the data due to nonelectronic decays of the τ lepton is determined by an iterative method based on the data itself. This minimizes the dependence of the result on assumptions about exclusive decay branching ratios, in particular, on the poorly measured hadronic decay modes involving neutrals.

A. Selection of radiative Bhabha and two-γ events

The shape of the electron peak was determined by studying radiative Bhabha events $e^+ e^- \rightarrow e^+ e^- (\gamma)$ and two-photon events $e^+ e^- \rightarrow e^+ e^- e^+ e^- (\gamma)$ (RBE), which were selected using a modification of the program written for the selection of the 1-1 τ-pair candidates. The following selection criteria were modified to enhance the fraction of RBE and suppress the τ-pair contamination.

(a) At least one track was required to be an electron

candidate, defined as having an associated shower energy $E > 3.0$ GeV or an E/p ratio > 0.5. This cuts rejects most μ-pair events and two-γ events with two μ's in the final state. It also substantially reduces the τ-pair contamination.

(b) The cut on the maximum total energy, as measured by the shower counters, was removed.

(c) The cut on the scalar sum of the charged-particle momenta was lowered from 7.25 to 2.0 GeV/c, which increases the statistics for low-momentum tracks coming mostly from two-γ events.

(d) The sum of the momenta transverse to the beam axis, $p_\perp$, was not allowed to exceed 1.0 GeV/c. This cut rejects a large fraction of the remaining τ pair events, but only reduces the number of RBE by about 50%. Figure 3 shows the $p_\perp$ distribution for events surviving the standard τ-pair event-selection criteria with modifications (a)–(c) and having the two tracks clearly identified as electrons by the χ_e^2 method described below. The distribution peaks strongly at zero transverse momentum in contrast to the distribution of Fig. 4, which was obtained from Monte Carlo–generated τ-pair events under the same conditions, but without the requirement on the number of electrons. The statistics in Fig. 4 corresponds to approximatively 2.5 times the integrated luminosity of the experiment.

(e) Track 1(2) of a given event was only accepted as an electron candidate if track 2(1) was clearly identified as an electron by the χ_e^2 method.

These RBE selection criteria results in 5774 tagged electrons. Their momentum distribution is shown in Fig. 5 where it is compared with the Monte Carlo–generated momentum distribution of electrons from the decay $\tau^- \rightarrow e^- \bar{\nu}_e \nu_\tau$, shown by the lines. The electrons from τ decay are normalized to the measured integrated luminosity of the experiment and have been subject to the standard τ-pair selection criteria. The curves correspond to an assumed branching ratio for the decay rate of the τ
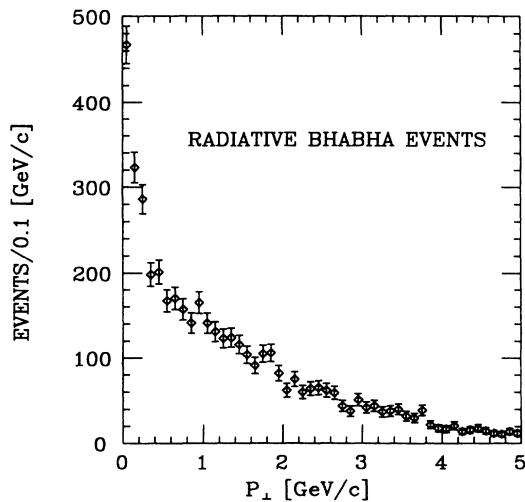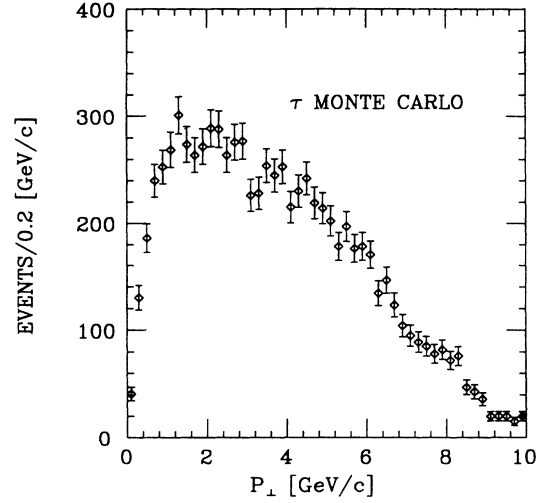

FIG. 4. Transverse-momentum distribution for Monte Carlo–generated τ-pair events selected as for Fig. 3, but without requiring two identified electrons.

lepton into electrons, B_e, of 18.0%. Although the RBE and τ decays have quite different distributions there are sufficient RBE over the full momentum interval.

B. E/p ratio

Figure 6 shows the E/p ratio for all one-prong τ decay candidates, in both the 1-1 [Fig. 6(a)] and 1-3 [Fig. 6(b)] charged-track topologies. Here E is the sum of the energies deposited in the module hit by the track and its two neighboring modules, and p is the track momentum. A clear peak is evident at $E/p = 1$ over a slowly falling background.

The shape of the electron signal from the $\tau \rightarrow e\nu\nu$ de-

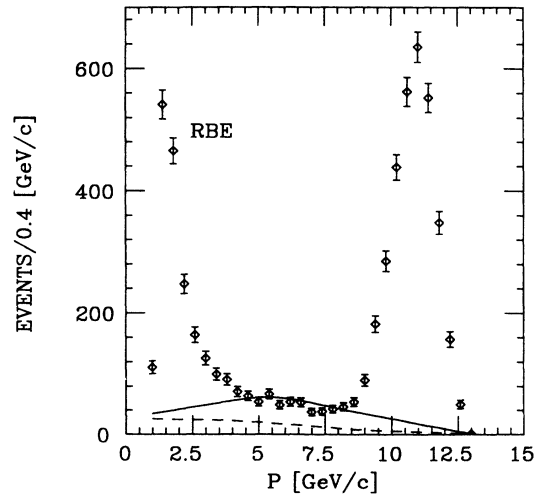FIG. 3. Transverse-momentum distribution for events with two clearly identified electrons.

FIG. 5. Momentum distribution of selected electron candidates. The solid (dashed) line corresponds to the expected spectrum for electrons from τ decay recoiling against one (three) charged particles. The normalizations are explained in the text.
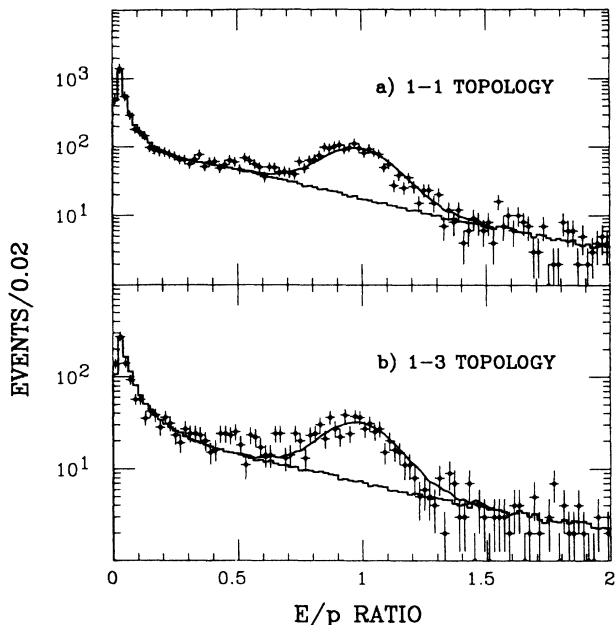
FIG. 6. Energy/momentum ratio for one-prong τ decays compared to the fits described in the text: (a) one-prong τ decays from the 1-1 decay topology, (b) one-prong τ decays from the 1-3 decay topology.

cays was simulated by weighting the RBE tracks according to the different momentum spectra of the electrons in the 1-1 and 1-3 τ-decay topology, as indicated by the lines in Fig. 5.[12]

The corrected E/p distributions for the 1-1 and 1-3 topologies, as shown in Fig. 7, were fitted to the sum of two

Gaussian distributions to determine the shape of the signal, $s(E/p)$. The relative normalization of the second Gaussian function is small. However, the fit is substantially improved by its inclusion, due to a better description of the tails.

In order to determine the form of the background in Fig. 6 from τ decays into all except the electronic modes, we used an iterative method based on event mixing. In a first iteration, the E/p distributions between 0.4 and 1.6 were fit[13] to a signal term $s(E/p)$ and an exponential function for the background:

$$f_0(E/p) = p_1 s(E/p) + p_2 b_0(E/p) ,\qquad (2)$$

where $b_0(E/p) = e^{-p_3 E/p}$ and p_i are free parameters. Then the background form was redetermined by calculating E/p using E for a given event, but using the momentum value from a different event. In order to avoid bias introduced by electrons in the sample, in the signal region of E/p from 0.4 to 1.6 only that fraction of events corresponding to the previously fitted background were used. This was done by selecting a random number x between 0 and $f_0(E/p)$ and accepting the energy E and the momentum p for mixing only if $x < p_2 b_0(E/p)$. High statistics for this estimation of the background was achieved by storing up to 500 momentum values for subsequent mixing.

In a second iteration, the data of Fig. 6 in the region from 0 to 2.0 were fitted bin by bin to the signal term and the newly obtained background $b_1(E/p)$:

$$f_1(E/p) = p_1 s(E/p) + p_2 b_1(E/p) ,\qquad (3)$$

where the normalizations p_i are the only free parameters and the event mixing was repeated with $f_1(E/p)$ and $p_2 b_1(E/p)$.

Figure 8 shows the number of electrons obtained after
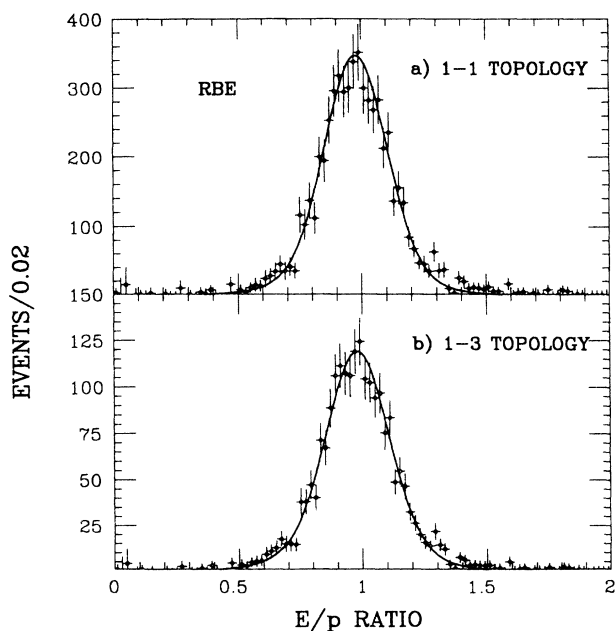

FIG. 7. Energy/momentum ratio for electrons from the decay $\tau \rightarrow e\nu\nu$ as simulated by RBE: (a) weighted according to the momentum spectrum of electrons in the 1-1 topology, (b) weighted according to the momentum spectrum of electrons in the 1-3 topology. The lines are explained in the text.
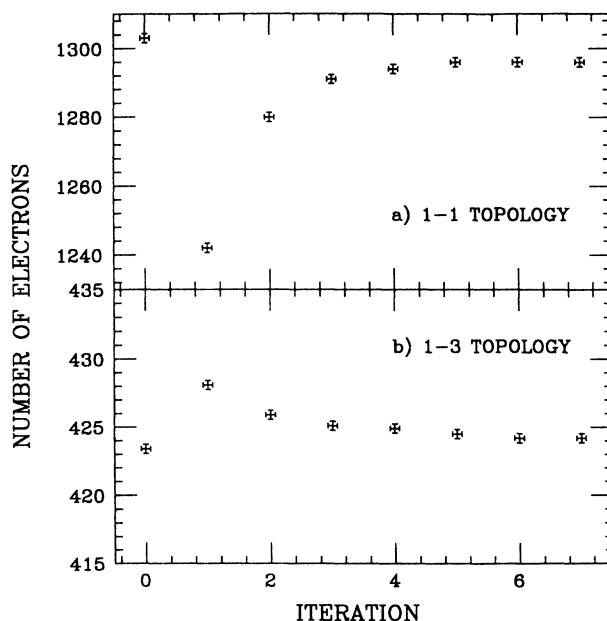

FIG. 8. Number of electrons obtained by the iterative method as a function of the number of iterations for the (a) 1-1 topology and (b) 1-3 topology.

the different iterations. After five iterations, the changes in the form of the background were negligible and the number of electrons remained constant. The resulting fit is shown in Fig. 6, the signal by the continuous line, and the background by the histogram.[14]

As an important check, this analysis technique was applied to τ-pair events generated by our Monte Carlo simulation. Fig. 9(a) shows the E/p distribution of the Monte Carlo–generated data selected with a 1-1 charged topology. The lines describing the signal and background were obtained with the iterative method in an identical way as for the real data. Figure 9(b) displays the E/p distribution for the background from all except the electronic τ decay modes in comparison with the background determined by the iterative method. The agreement between the known input and the result of the iterative method for both the number of electrons and the background shape is excellent. However, this check is not sensitive to the shape of the electron signal as determined by the RBE, since we use a parametrization of the signal generated by the Monte Carlo simulation of the experiment.

C. χ^2 technique

We define a χ^2 for a track to be an electron in the following way:

$$\chi_e^2 = \left| \frac{E_3 - \bar{E}_3(p)}{\sigma_{E_3}} \right|^2 + \left| \frac{E_8 - \bar{E}_8(p)}{\sigma_{E_8}} \right|^2 , \qquad (4)$$

where E_3 (E_8) is the energy in GeV measured by the front $3X_0$ (rear $8X_0$) section of the calorimeter. The average energy deposited in the front and rear section as a

FIG. 10. χ_e^2 distribution for electrons from the decay $\tau \to e\nu\nu$ as simulated by RBE: (a) weighted according to the momentum spectrum of electrons in the 1-1 topology, (b) weighted according to the momentum spectrum of electrons in the 1-3 topology. The lines are explained in the text.

function of track momentum was measured by the RBE and parametrized as follows:

$$\bar{E}_3(p) = (0.17 + 0.43 e^{-0.36p})p , \qquad (5)$$

$$\bar{E}_8(p) = p - \bar{E}_3(p) .$$

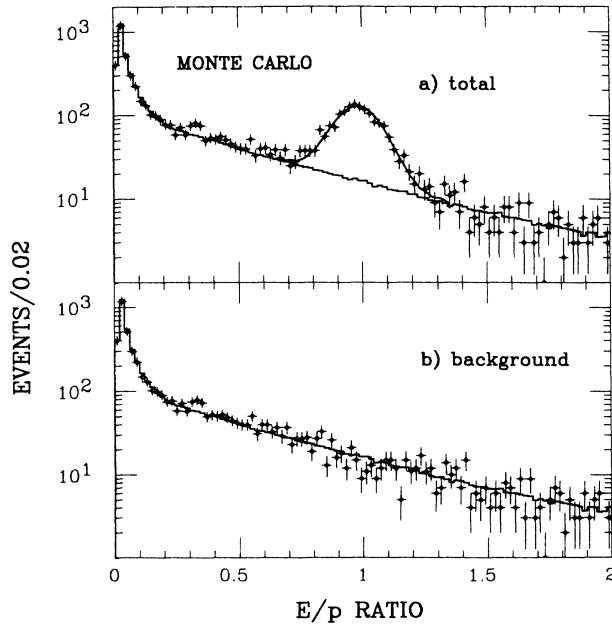The energy resolution, as a function of deposited ener-

FIG. 9. Energy/momentum ratio for one-prong τ decays with a 1-1 charged topology generated by Monte Carlo simulation compared to the fits described in the text: (a) all decay modes, (b) all decay modes except the decays into electrons.
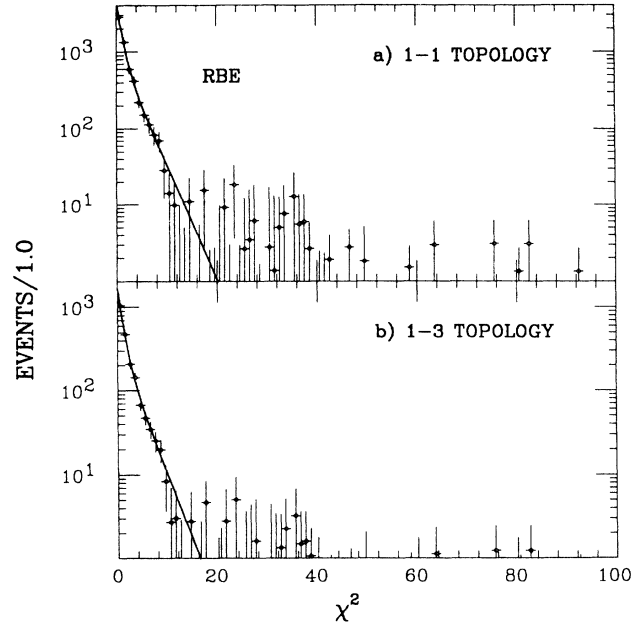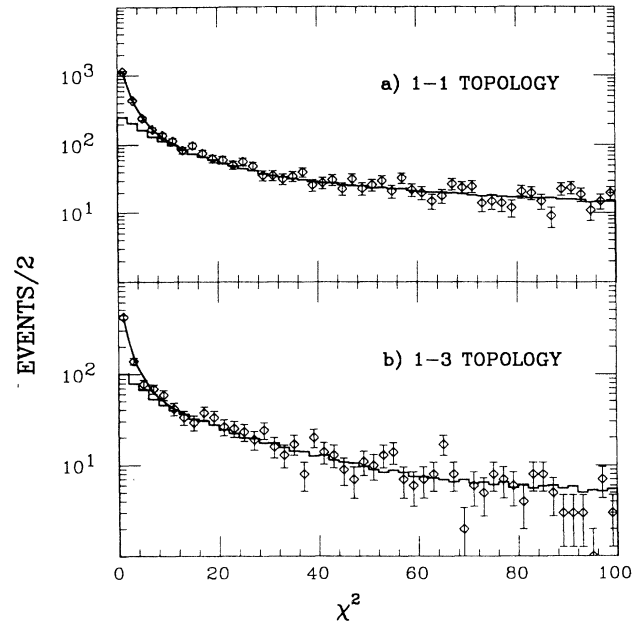
FIG. 11. Distribution in χ_e^2 [Eq. (2)] compared to the fits described in the text: (a) one-prong τ decays from the 1-1 decay topology, (b) one-prong τ decays from 1-3 decay topology.

TABLE I. Summary of results.

| Topology | Number of electrons | | Background | Detection efficiencies | $B(\tau \to e\nu\nu)$ |
	E/p method	χ_e^2 method			
1-1	1296±42	1288±43	154±20	8.49%	(16.9±0.6)%
1-3	424±25	423±27	1±1	3.10%	(17.2±1.0)%
Total	1720±49	1711±51	155±20	11.59%	(17.0±0.5)%

gy for the two sections separately, was determined from the RBE events and is well described by

$$\sigma_{E_3} = 37.5\sqrt{E_3} \% ,$$

$$\sigma_{E_8} = 46.1\sqrt{E_8} \% . \qquad (6)$$

Using these parametrizations, the expected χ_e^2 distributions for electrons in the 1-1 and 1-3 τ-decay topologies were separately determined. The τ-pair background in the RBE sample was again subtracted as for the E/p signal and the distributions were fitted to the sum of two exponentials, as shown in Fig. 10.[15]

Figure 11 shows the χ_e^2 distributions for the τ data. The backgrounds under the electron signals at low χ_e^2 are mostly due to the overlap of charged pions with photons from decays such as $\tau^- \to \rho^- \nu_\tau \to \pi^- \pi^0 \nu_\tau$.

The shape of the background was determined in an analogous way to the E/p method, by mixing E_3 and E_8 from one event with the momentum from another event. After five iterations the change in the background forms and the number of electrons were negligible and the procedure was stopped. The resulting signals are shown as the solid lines and the backgrounds as the histograms in Fig. 11.

This method has also been applied to Monte Carlo–generated τ-pair events. Again, both the number of electrons and the shape of the background have been accurately reconstructed.

D. Results

The number of electrons obtained by the two analyses, using the E/p ratio and the χ_e^2 method, are in excellent agreement, as shown in Table I.

V. BACKGROUNDS TO THE ELECTRON SIGNALS FROM NON-τ-PAIR EVENTS

The backgrounds in the 1-1 sample both from two-γ events $e^+e^- \to e^+e^-e^+e^-(\gamma)$ and from radiative Bhabha events were determined by studying the distribution in transverse momentum $p_\perp$ for events in which both tracks were consistent with being electrons. Figure 12 shows the $p_\perp$ distribution for 1-1 τ-pair events selected requiring for both tracks:

$$0.4 < (E/p)_i < 1.6, \quad i = 1,2 .$$

The distribution shows an enhancement at low $p_\perp$ values in contrast with the prediction of the τ Monte Carlo simulation. The shape of the enhancement has been determined with the RBE. The RBE were selected

with identical 1-1 τ-pair selection criteria, except for the following modifications: (a) at least one track was required to be an electron candidate, defined as having an associated shower energy $E > 3.0$ GeV or an E/p ratio > 0.5; (b) both tracks were required to be good electron candidates with $\chi_e^2 < 10$.

Two corrections were applied to the $p_\perp$ distribution of the RBE. First, the background from τ-pair events, here determined by applying identical selection criteria to Monte Carlo–generated events, was subtracted. Second, the $p_\perp$ distribution was corrected for the effect on the efficiency due to modification (a) of the standard τ-pair selection criteria. This was done by comparing the effect of modification (a) on the $p_\perp$ distribution of Monte Carlo–generated τ-pair events. Finally, the corrected $p_\perp$ distribution of the RBE were fitted empirically to a Breit-Wigner distribution.

The data of Fig. 12 are fitted to the parametrized contribution from the RBE and the prediction by the τ-pair Monte Carlo simulation. The fraction of RBE corresponds to 77±10 events or 154±20 electrons, where the error includes the effects of the background shape determination as well as the uncertainty of the fit.

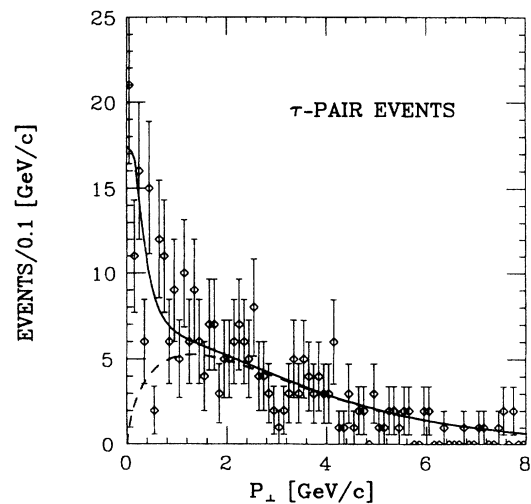The background in the 1-3 sample was determined by searching for events containing a e^+e^- pair, in addition

FIG. 12. $p_\perp$ distribution for selected 1-1 τ pairs, where both tracks are compatible with being electrons. The lines represent the result of the fit: The solid line shows the background from two-γ events and radiative Bhabha events, and the dashed line corresponds to the τ-pair events.

to a converted photon. Only one background candidate was found.

VI. EFFICIENCY CALCULATIONS AND RESULTS FOR THE BRANCHING RATIO FOR
$$\tau^- \to e^- \bar{v}_e v_\tau$$

The branching ratio $B_{e_j} = B(\tau \to e v v)_j$ for the 1-j charged topology data sample is calculated as

$$B_{e_j} = \frac{N_{e_j}}{\epsilon_j N_\tau} , \qquad (7)$$

where the N_τ, number of τ leptons produced is given by

$$N_\tau = 2\sigma_{\tau\tau_{\text{rad}}} \int L \, dt = 79\,477 ,$$

and N_{e_j} is the background-corrected number of electrons recoiling against j charged tracks.

The efficiencies ϵ_j for detecting the $\tau \to e v v$ decays recoiling against a τ decay with charged topology j were obtained from a Monte Carlo simulation of τ production and decay, which includes α^3 QED radiative corrections[16] and full detector simulation. The efficiencies ϵ_j are somewhat dependent on the exact exclusive branching ratios. As an example, the τ event-selection criteria suppress events where electrons recoil against ρ mesons relative to events where electrons recoil against μ's. Therefore, we calculated the efficiencies for each recoil mode i separately:

$$\epsilon_1^i = \frac{N_1^{i^+} + N_1^{i^-}}{N_{\text{gen}}}, \quad \text{for 1-1 events} ,$$

$$\epsilon_3^i = \frac{N_3^i}{N_{\text{gen}}}, \quad \text{for 1-3 events} , \qquad (8)$$

where $N_1^{i^+}$ ($N_1^{i^-}$) is the number of selected Monte Carlo–generated τ-pair events with an electron that recoils against a positively (negatively) charged τ lepton decaying into mode i.

These differential efficiencies are weighted by a set of ratios of chosen branching ratios B_{chosen}^i and branching ratios used by the event generator B_{MC}^i,

$$\epsilon_{j_{\text{weight}}}^i = \epsilon_j^i \frac{B^i}{B_{\text{MC}}^i} , \qquad (9)$$

and summed up to give the overall efficiencies for a given topology:

$$\epsilon_j = \sum_i \epsilon_{j_{\text{weight}}}^i . \qquad (10)$$

Several different sets of conceivable values for the B_{chosen}^i were used and the final efficiencies were determined as the average values of the corresponding efficiencies. The numbers for the average efficiencies are displayed in Table I, together with the results for B_{e_j}.
The final result and statistical error for the branching ratio for the decay $\tau \to e v v$ is $B_e = (17.0 \pm 0.5)\%$.

VII. DISCUSSION OF SYSTEMATIC ERRORS

The following contributions to the systematic error were considered.

(a) The result depends strongly on the parametrization of the electron signals in the E/p and χ_e^2 distributions, in particular on a precise description of the tails. Because of the high statistics of the RBE sample, the shape of the signals were well determined. A generous variation of these shapes resulted in a change of $\pm 0.3\%$ on B_e. The dependence of the result on the exact functions used for the average energy deposited in the inner three and outer eight radiation length of the shower counter Eq. (5) as well as their errors Eq. (6) was negligible.

The difference of about a factor of 4 in the final-state radiation of the Bhabha events as compared to the τ-pair events will cause a relative shift in the E/p distributions of the two samples. This is because the energy of photons from final-state radiation is in general deposited in the calorimeter close to the point at which the electrons deposit energy and is, therefore, included in the calorimeter energy measurement. A Monte Carlo simulation shows that without a cut in the transverse momentum for RBE the central value of the electron signal shifts upwards by $\sim 1\%$. However, the cut in transverse momentum at 1 GeV/c applied when selecting RBE, reduces this effect to a negligible level.

(b) The uncertainty in the measured integral luminosity and the fraction of background from radiative Bhabha events and two-γ events contribute errors of $\pm 0.3\%$ and $\pm 0.2\%$.

(c) There are three contributions to the uncertainty in the efficiency calculation. The efficiency for selecting τ-pair candidates depends on a proper simulation of the response of the barrel shower-counter system. This uncertainty contributes an error of $\pm 0.2\%$, mostly due to the uncertainty in the rejection of τ-pair events where both τ leptons decay into electrons. Finally, the uncertainties in the exclusive one-prong decay branching ratios
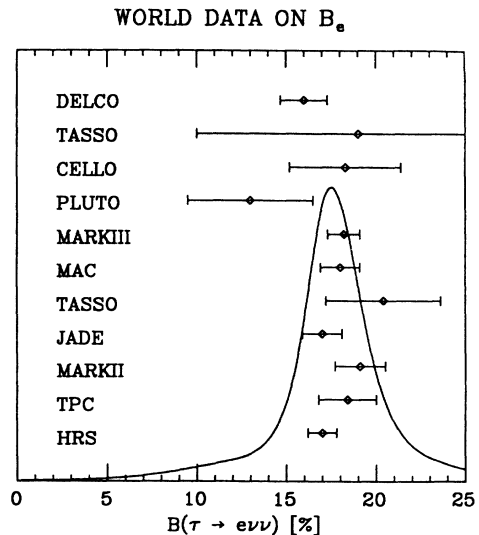

WORLD DATA ON B_e

FIG. 13. World data for all direct measurements of B_e.

and the limited statistics of the Monte Carlo simulation gave error contributions of ±0.2% and ±0.1%, respectively.

(d) The result was insensitive to modifications of the fiducial cut on the lateral incident position of the tracks onto the barrel shower-counter modules.

These contributions to the systematic error on B_e are independent and so were added in quadrature to yield a total systematic error of ±0.6%. The final result is then $B_e = (17.0\pm0.5\pm0.6)\%$, where the first error is statistical and the second systematic.

Our value is in good agreement with the world-average value of all previous direct measurements[17] of $B_e = (17.8\pm0.5)\%$. Figure 13 shows the results of all published direct measurements of B_e. The errors have been compiled by adding the quoted statistical and systematic errors in quadrature. The ideogram displayed in Fig. 13 is drawn as proposed by the Particle Data Group and corroborates that all direct measurements give consistent results. The new world-average value, including the present measurement is $B_e = (17.6\pm0.4)\%$.

VIII. COMPARISON TO THEORETICAL EXPECTATIONS

Using non-τ data, most of the exclusive decay branching ratios of the τ lepton can be related to the rate for $\tau \rightarrow e\nu\nu$. Table II shows the theoretical expectations[18] for the ratios $R_i = B_i/B_e$, where B_i is any exclusive τ decay branching ratio.

Four comments are in order here.

(a) The uncertainty on the sum of decay modes leading to a one-charged prong topology is dominated by the uncertainty in R_ρ, which is related to the absolute normalization of the measurement of the cross section for $e^+e^- \rightarrow \pi^+\pi^-$ below the τ mass.

(b) No reliable theoretical prediction for $B_{(\pi\pi\pi)^-}$ is available. Following the experimental evidence that this final state proceeds dominantly via the $a_1(1260)$ resonance, we have set the contributions to the 1- and 3-prong final states equal.

(c) There is no prediction or useful upper limit for the rate of $\tau^- \rightarrow 2\pi^-\pi^+2\pi^0$.

(d) The rest includes rare decays such as $\tau^- \rightarrow (5\pi)^-\nu$, $(K\pi\pi)^-\nu$, $(\eta\pi\pi)^-\nu$, etc. Note that their contribution to the sum is small compared to the overall error.

Using the total rates for the one- and three-prong topology of Table II, we can set up the following sets of equations:

$$B_1 = [(4.00\pm0.12)+0.5R_{(\pi\pi\pi)^-}]B_e \ ,$$
$$B_3 = [(0.29\pm0.06)+0.5R_{(\pi\pi\pi)^-} + R_{2\pi^-\pi^+2\pi^0}]B_e \ . \quad (11)$$

Neglecting $R_{2\pi^-\pi^+2\pi^0}$, our measured values for the topological branching fractions[11] of

$$B_{1_{HRS}} = (86.4\pm0.3\pm0.3)\% \ ,$$

and   (12)

$$B_{3_{HRS}} = (13.5\pm0.3\pm0.3)\%$$

yield

$$B_e^t = (19.6\pm0.8)0004$$

and   (13)

$$B_{(\pi\pi\pi)^-} = (15.6\pm2.7)\% \ ,$$

where the errors are dominated by the error on R_ρ. Note that if there is a substantial fraction of the decays $\tau^- \rightarrow (\pi\pi\pi)^-\nu$, which do not proceed via the $a_1(1260)$ resonance and/or $R_{2\pi^-\pi^+2\pi^0}$ is significantly different from zero, the value for B_e^t would increase, while the value for $B_{(\pi\pi\pi)^-}$ would decrease.

Assuming lepton universality, the τ lifetime is related to the leptonic decay branching ratio through the equation

$$B_e = \frac{\tau_\tau}{\tau_\mu}\left[\frac{m_\tau}{m_\mu}\right]^5 \quad (14)$$

where $\tau_{\mu,\tau}$ and $m_{\mu,\tau}$ are the lifetimes and masses of the μ and τ leptons.

We have measured the flight distances of 1311 τ decays

TABLE II. Theoretical predictions for the ratio of exclusive τ decay modes to $B(\tau \rightarrow e\nu\nu)$. CVC denotes the conserved-vector-current hypothesis.

Decay	1-prong topology	3-prong topology	Input
$e^-\nu\nu$	1.00	0.0	
$\mu^-\nu\nu$	0.973	0.0	Phase space
$\pi^-\nu$	0.601	0.0	τ_π
$K^-\nu$	0.0395	0.0	τ_K
$(\pi\pi)^-\nu$	1.26±0.12	0.0	CVC, $\sigma(e^+e^- \rightarrow \pi^+\pi^-)$
$(K\pi)^-\nu$	$\frac{7}{9}(0.057\pm0.009)$	$\frac{2}{9}(0.057\pm0.009)$	CVC, $\sigma(e^+e^- \rightarrow \pi^+\pi^-)$,
			Cabibbo angle
$(\pi\pi\pi)^-\nu$	$\frac{1}{2}R_{(\pi\pi\pi)^-}$	$\frac{1}{2}R_{(\pi\pi\pi)^-}$	No prediction
$(4\pi)^-\nu$	0.056±0.006	0.251±0.060	CVC, $\sigma(e^+e^- \rightarrow 4\pi)$
Rest	0.02±0.02	$(0.03\pm0.02)+R_{2\pi^-\pi^+2\pi^0}$	Experiment and Theory
Total	(4.00 ± 0.12) $+0.5R_{(\pi\pi\pi)^-}$	(0.29 ± 0.06) $+0.5R_{(\pi\pi\pi)^-} + R_{2\pi^-\pi^+2\pi^0}$	

TABLE III. Comparison of different measurements of B_e.

Method	B_e	Difference with B_e^l	Significance
Direct measurement (B_e)	$(17.0\pm0.8)\%$	$(2.6\pm1.1)\%$	2.3σ
Lifetime measurement (B_e^τ)	$(18.7\pm1.1)\%$	$(0.9\pm1.3)\%$	0.7σ
Average (B_e,B_e^τ)	$(17.7\pm0.7)\%$	$(1.9\pm1.1)\%$	1.8σ
Topological branching fraction (B_e^l)	$(19.6\pm0.8)\%$		
Average (B_e,B_e^τ,B_e^l)	$(18.5\pm0.5)\%$		

to three charged particles using a four-layer tubular cell vertex chamber in conjunction with the main drift chamber and find a τ lifetime[19] of $\tau_\tau=(2.99\pm0.15\pm0.10)\times10^{-13}$ s.

Applying Eq. (14) to our lifetime measurements gives

$$B_e^\tau=(18.7\pm0.9\pm0.6)\% . \qquad (15)$$

Table III compares our different determinations of B_e. The agreement between the direct measurement B_e and the measurement via the topological branching fractions B_e^l is poor: The discrepancy corresponds to 2.3 standard deviations. Ignoring these differences and averaging the three determinations yields $B_e=(18.8\pm0.5)\%$.

IX. CONCLUSIONS

We report the measurement of the decay rate into electrons of the τ lepton, $B_e=(17.0\pm0.5\pm0.6)\%$. We compare the result with theoretical expectations based on our measurements of the lifetime and topological branching fractions of the τ lepton and observe an inconsistency at the level of two standard deviations. Other groups[2] have observed similar inconsistencies, but caution has to be applied when combining results from different experiments. Specifically, a recent statistical analysis[20] of the global measurements of the exclusive τ decay channels show evidence for bias. Therefore, conclusions about the confidence level of discrepancies that rest on the use of world-average measurements are suspect. We conclude that the inconsistency in τ decay is not significant enough to cast serious doubt on the standard model of electroweak interactions. However, a dedicated high-statistics experiment with emphasis on the measurement of τ decay modes involving neutral particles is strongly needed.

ACKNOWLEDGMENTS

*Present address: Fermi National Accelerator Laboratory, Batavia, IL 60510.

†Present address: NIKHEF-H, Amsterdam, The Netherlands.

‡Present address: CRN Division de Hautes Energies, Strasbourg, France.

§Present address: Stanford Linear Accelerator Center, Stanford, CA 94305.

**Present address: University of Wisconsin, Madison, WI 53706.

††Present address: University of Kansas, Lawrence, KS 66045.

‡‡Present address: Ohio State University, Columbus, OH 43210.

§§Present address: Virginia Polytechnic Inst. and State University, Blacksburg, VA 24061.

[1] M. L. Perl, Phys. Rev. Lett. 35, 1489 (1975).

[2] B. C. Barish and R. Stroynowski, Phys. Rep. 157, 1 (1988); K. K. Gan and M. L. Perl, Int. J. Mod. Phys. A 3, 531 (1988).

[3] H.-J. Gerber, in Proceedings of the International Europhysics Conference on High Energy Physics, Uppsala, Sweden, 1987, edited by O. Bottner (European Physical Society, Petit-Lancy, Switzerland, 1987).

[4] T. N. Truong, Phys. Rev. D 30, 1509 (1984).

[5] K. Hayes, talk presented at the Tau-Charm Factory Workshop, Stanford Linear Accelerator, Stanford, California, 1989 (unpublished).

[6] Independent of dynamics, isotopic-spin conservation forces

$$B(\tau^-\to\pi^-\pi^0\pi^0)\le B(\tau^-\to\pi^-\pi^+\pi^-) .$$

[7] S. Abachi et al., Phys. Lett. B 226, 405 (1989).

[8] D. Bender et al., Phys. Rev. D 30, 515 (1984); G. Baranko et al., Nucl. Instrum. Methods 169, 413 (1980); D. Rubin et al., ibid. 203, 119 (1982); P. Baringer et al., ibid. A254, 542 (1987).

[9] J. S. Loos, Nucl. Instrum. Methods A249, 185 (1986).

[10] M. Derrick et al., Phys. Rev. D 34, 3286 (1986).

[11] S. Abachi et al., Phys. Rev. D 40, 902 (1989).

[12] The small background from τ-pair events in the RBE sample, where at least one τ decays into an electron, was determined by applying the RBE selection criteria to the Monte Carlo–generated τ-pair events. The resulting normalized E/p distributions were subtracted from the RBE signal.

[13] As the content of some bins is below eight counts, we have fitted the data using a maximum-likelihood method with Poisson error distributions.

[14] A better fit can be obtained by allowing the central value of the signal peak to shift downwards. This results in a substantially larger signal fraction. However, as we have used identical programs for the analysis of the RBE and τ-pair events, except for the modification of some selection criteria, the peak position is fixed in the fit. Both data samples are pro-

cessed with identical calibration constants for the barrel shower-counter system and tracking detector.

[15]After the subtraction of the τ-pair background the sum over all entries above a χ_e^2 of 20 is consistent with zero. Therefore, we did not include a third exponential function to describe the signal shape.

[16]F. A. Berends and R. Kleiss, Nucl. Phys. **B177**, 237 (1981); F. A. Berends, R. Kleiss, and S. Jadach, *ibid.* **B202**, 63 (1982).

[17]Particle Data Group, G. P. Yost *et al.*, Phys. Lett. B **204**, 1 (1988).

[18]F. J. Gilman and S. H. Rhie, Phys. Rev. D **31**, 1066 (1985); F. J. Gilman, *ibid.* **35**, 3541 (1987); W. J. Marciano and A. Sirlin, Phys. Rev. Lett. **61**, 1815 (1988).

[19]S. Abachi *et al.*, Phys. Rev. Lett. **59**, 2519 (1987).

[20]K. G. Hayes and M. L. Perl, Phys. Rev. D **38**, 335 (1988).